Weak interactions in polarized semi-inclusive DIS

M. Anselmino[1], M. Boglione[2], U. D'Alesio[3], F. Murgia[3]

[1] Dipartimento di Fisica Teorica, Università di Torino and INFN, Sezione di Torino, Via P. Giuria 1, 10125 Torino, Italy
[2] Department of Physics, University of Durham, Science Laboratories, South Road, Durham DH11 3LE, UK
[3] INFN, Sezione di Cagliari and Dipartimento di Fisica, Università di Cagliari, C.P. 170, 09042 Monserrato (CA), Italy

Abstract. We calculate, within the pQCD parton model at leading orders, the expression of the polarization P of spin 1/2 hadrons (typically Λ baryons), produced in polarized semi-inclusive DIS in all possible cases in which weak interactions are involved. We discuss how to gather new information on fragmentation and distribution functions and give numerical estimates in the cases for which data are or will soon be available.

1 Introduction

The polarization of spin 1/2 baryons inclusively produced in polarized deep inelastic scattering processes may be useful, if measurable, to obtain new information on polarized distribution and fragmentation functions. A lot of attention has recently been paid to the self-revealing polarization of Λ's and other hyperons [1–12]. Most papers, with the exception of [5,8] and [11], do not consider weak interaction contributions, due to lack of available experimental information.

The NOMAD collaboration have recently published some very interesting results [13] on the Λ polarization in ν_μ charged current interactions; more data might soon be available from high energy neutral current processes at HERA, due to electro-weak interference effects. It is then appropriate and timely to perform a systematical and comprehensive study of weak interaction contributions to the production and the polarization of baryons in as many as possible DIS processes. We stress that such contributions are an important source of new information, due to the natural neutrino polarization and to the selected couplings of W's to pure helicity states.

We consider weak interactions in the following processes:

$$\nu p \to \ell^- \Lambda^\uparrow + X \quad \text{(charged current)},$$
$$\bar\nu p \to \ell^+ \Lambda^\uparrow + X \quad \text{(charged current)},$$
$$\ell^- p \to \nu \Lambda^\uparrow + X \quad \text{(charged current)},$$
$$\ell^+ p \to \bar\nu \Lambda^\uparrow + X \quad \text{(charged current)},$$
$$\nu p \to \nu \Lambda^\uparrow + X \quad \text{(neutral current)},$$
$$\bar\nu p \to \bar\nu \Lambda^\uparrow + X \quad \text{(neutral current)},$$
$$\ell p \to \ell \, \Lambda^\uparrow + X \quad \text{(neutral current)},$$

where the lepton ℓ and the proton p may or may not be polarized, whereas the neutrinos are obviously always polarized ($\lambda_\nu = -1/2$, $\lambda_{\bar\nu} = +1/2$).

In our calculations we take into account the leading twist factorization theorem, standard model elementary interactions at lowest perturbative order and LO QCD evolution only. Consequently the cross-sections for the production of a hadron B in the current fragmentation region are given by

$$\frac{\mathrm{d}\sigma}{\mathrm{d}x\mathrm{d}y\mathrm{d}z} = \sum_q q(x, Q^2)\frac{\mathrm{d}\hat\sigma}{\mathrm{d}y}D_{B/q}(z, Q^2), \qquad (1)$$

where $q(x,Q^2)$ is the quark q distribution function, $D_{B/q}(z,Q^2)$ is the fragmentation function of the quark in the detected hadron B, and $\mathrm{d}\hat\sigma/\mathrm{d}y$ is the elementary cross-section. The usual DIS variables x, y and z are defined by $x = Q^2/2p \cdot q$, $y = q \cdot p/\ell \cdot p$ and $z = p_B \cdot p/p \cdot q$ (see also Appendix B).

In Sects. 2–4 we consider separately the different processes, and derive explicit expressions for the polarization of a final baryon B in terms of elementary dynamics, quark distribution and fragmentation functions. In Sect. 5 we discuss how experimental data could be used to obtain specific new information and give predictions for several processes which might be of interest in the near future. In Appendix A we give full information on the kinematical ranges and configurations for each of the experiments in progress or planned, used to derive our numerical results. In Appendix B we discuss mass effects in the fragmentation process, to clarify differences and relationships between different definitions of the variable on which the fragmentation functions depend.

2 Charged current processes, $\nu p \to \ell \Lambda^\uparrow \, X$ and $\ell p \to \nu \Lambda^\uparrow \, X$

Let us consider first the neutrino initiated processes, $\nu p \to \ell \Lambda^\uparrow X$; for them, there exist 4 possible elementary contributions, corresponding to the interactions

$$\nu d_j \to \ell^- u_i,$$
$$\nu \bar{u}_i \to \ell^- \bar{d}_j,$$
$$\bar{\nu} u_i \to \ell^+ d_j,$$
$$\bar{\nu} \bar{d}_j \to \ell^+ \bar{u}_i \,, \tag{2}$$

where we use the notation

$$u_i = u, c, \quad d_j = d, s. \tag{3}$$

Neglecting quark masses one finds that there is only one non-zero helicity amplitude $\hat{M}_{\lambda_\ell, \lambda_{q_i}; \lambda_\nu, \lambda_{q_j}}$ for each of the elementary processes in (2), and precisely

$$\hat{M}^{\nu d_j \to \ell^- u_i}_{--;--} = \hat{M}^{\bar{\nu} \bar{d}_j \to \ell^+ \bar{u}_i}_{++;++} = -\frac{4\pi\alpha V_{ij}}{\sin^2\theta_W} \frac{1}{y + M_W^2/xs}, \tag{4}$$

$$\hat{M}^{\nu \bar{u}_i \to \ell^- \bar{d}_j}_{-+;-+} = \hat{M}^{\bar{\nu} u_i \to \ell^+ d_j}_{+-;+-} = -\frac{4\pi\alpha V_{ij}}{\sin^2\theta_W} \frac{1-y}{y + M_W^2/xs}, \tag{5}$$

where, according to the usual SM rules,

$$V_{ud} = V_{cs} = \cos\theta_C \quad V_{us} = -V_{cd} = \sin\theta_C; \tag{6}$$

θ_W is the Weinberg angle, θ_C is the Cabibbo angle and $V_{ij} = V_{ji}^*$.

The elementary cross-sections are computed according to

$$\frac{d\hat{\sigma}_{\lambda\lambda'}}{dQ^2} = \frac{1}{16\pi x^2 s^2} |\hat{M}_{\lambda\lambda';\lambda\lambda'}|^2 = \frac{1}{sx} \frac{d\hat{\sigma}_{\lambda\lambda'}}{dy}, \tag{7}$$

from which we obtain

$$\frac{d\hat{\sigma}^{\nu d_j \to \ell^- u_i}_{--}}{dy} = \frac{d\hat{\sigma}^{\bar{\nu} \bar{d}_j \to \ell^+ \bar{u}_i}_{++}}{dy}$$
$$= \frac{\pi\alpha^2}{xs} \frac{|V_{ij}|^2}{\sin^4\theta_W} \left(\frac{1}{y + M_W^2/xs} \right)^2, \tag{8}$$

$$\frac{d\hat{\sigma}^{\nu \bar{u}_i \to \ell^- \bar{d}_j}_{-+}}{dy} = \frac{d\hat{\sigma}^{\bar{\nu} u_i \to \ell^+ d_j}_{+-}}{dy}$$
$$= \frac{\pi\alpha^2}{xs} \frac{|V_{ij}|^2}{\sin^4\theta_W} \left(\frac{1-y}{y + M_W^2/xs} \right)^2. \tag{9}$$

Notice that both ν and $\bar{\nu}$ couple only to quarks with negative helicity and antiquarks with positive helicity.

We can now compute the longitudinal polarizations $P_{[\nu,\ell]}$ and $P_{[\bar{\nu},\ell]}$ for any spin 1/2 baryon B (Λ's and $\bar{\Lambda}$'s for instance) produced in neutrino initiated, charged current DIS scattering processes:

$$P_{[\nu,\ell]}(B) = \frac{d\sigma^{\nu p \to \ell^- B_+ X} - d\sigma^{\nu p \to \ell^- B_- X}}{d\sigma^{\nu p \to \ell^- B_+ X} + d\sigma^{\nu p \to \ell^- B_- X}} \tag{10}$$

and

$$P_{[\bar{\nu},\ell]}(B) = \frac{d\sigma^{\bar{\nu} p \to \ell^+ B_+ X} - d\sigma^{\bar{\nu} p \to \ell^+ B_- X}}{d\sigma^{\bar{\nu} p \to \ell^+ B_+ X} + d\sigma^{\bar{\nu} p \to \ell^+ B_- X}}, \tag{11}$$

where $B_\pm$ denotes a baryon B with helicity $\pm$.

In the most general case, when also the proton p is polarized – and we denote by an S in the superscript its spin state – from (1), (10) and (11) we obtain

$$P^{(S)}_{[\nu,\ell]}(B) = -\left(\sum_{i,j} \left[(d_j)^{(S)}_- d\hat{\sigma}^{d_j \to u_i}_{--} \Delta D_{B/u_i} \right. \right.$$
$$\left. - (\bar{u}_i)^{(S)}_+ d\hat{\sigma}^{\bar{u}_i \to \bar{d}_j}_{-+} \Delta D_{B/\bar{d}_j} \right] \Big/$$
$$\left(\sum_{i,j} \left[(d_j)^{(S)}_- d\hat{\sigma}^{d_j \to u_i}_{--} D_{B/u_i} \right. \right.$$
$$\left. \left. + (\bar{u}_i)^{(S)}_+ d\hat{\sigma}^{\bar{u}_i \to \bar{d}_j}_{-+} D_{B/\bar{d}_j} \right] \right) \tag{12}$$

and

$$P^{(S)}_{[\bar{\nu},\ell]}(B) = -\left(\sum_{i,j} \left[(u_i)^{(S)}_- d\hat{\sigma}^{u_i \to d_j}_{+-} \Delta D_{B/d_j} \right. \right.$$
$$\left. - (\bar{d}_j)^{(S)}_+ d\hat{\sigma}^{\bar{d}_j \to \bar{u}_i}_{++} \Delta D_{B/\bar{u}_i} \right] \Big/$$
$$\left(\left[(u_i)^{(S)}_- d\hat{\sigma}^{u_i \to d_j}_{+-} D_{B/d_j} \right. \right.$$
$$\left. \left. + (\bar{d}_j)^{(S)}_+ d\hat{\sigma}^{\bar{d}_j \to \bar{u}_i}_{++} D_{B/\bar{u}_i} \right] \right), \tag{13}$$

where an expression like $(q)^{(S)}_\pm$ stands for the number density (distribution function) of quarks q with helicity $\pm$ inside a proton with spin S, whereas $q_\pm$ alone refers, as usual, to a proton with $+$ helicity. The polarized fragmentation functions are defined as

$$\Delta D_{B/q} \equiv D_{B_+/q_+} - D_{B_-/q_+} = D_{B_-/q_-} - D_{B_+/q_-}. \tag{14}$$

If we now explicitly perform the sum over flavors in the numerators and denominators of (12) and (13), neglecting c quark contributions, and use (8) and (9), we obtain for longitudinally ($\pm$ helicity) polarized protons

$$P^{(\pm)}_{[\nu,\ell]}(B; x, y, z) = -\left([d_\mp + R s_\mp] \Delta D_{B/u} \right.$$
$$\left. - (1-y)^2 \bar{u}_\pm \left[\Delta D_{B/\bar{d}} + R \Delta D_{B/\bar{s}} \right] \right) \Big/$$
$$\left([d_\mp + R s_\mp] D_{B/u} \right.$$
$$\left. + (1-y)^2 \bar{u}_\pm \left[D_{B/\bar{d}} + R D_{B/\bar{s}} \right] \right) \tag{15}$$

and

$$P^{(\pm)}_{[\bar{\nu},\ell]}(B; x, y, z) = \left([\bar{d}_\pm + R \bar{s}_\pm] \Delta D_{B/\bar{u}} \right.$$
$$\left. - (1-y)^2 u_\mp \left[\Delta D_{B/d} + R \Delta D_{B/s} \right] \right) \Big/$$
$$\left([\bar{d}_\pm + R \bar{s}_\pm] D_{B/\bar{u}} \right.$$
$$\left. + (1-y)^2 u_\mp \left[D_{B/d} + R D_{B/s} \right] \right), \tag{16}$$

where $R \equiv \sin^2\theta_{\mathrm{C}}/\cos^2\theta_{\mathrm{C}} \simeq 0.056$.

In the simpler case in which the proton is unpolarized one replaces q_+ and q_- with $q/2$ so that (15) and (16) become respectively

$$P_{[\nu,\ell]}^{(0)}(B;x,y,z) \tag{17}$$
$$= -\frac{[d+Rs]\Delta D_{B/u} - (1-y)^2\bar{u}[\Delta D_{B/\bar{d}} + R\Delta D_{B/\bar{s}}]}{[d+Rs]D_{B/u} + (1-y)^2\bar{u}[D_{B/\bar{d}} + RD_{B/\bar{s}}]}$$

and

$$P_{[\bar{\nu},\ell]}^{(0)}(B;x,y,z) \tag{18}$$
$$= \frac{[\bar{d}+R\bar{s}]\Delta D_{B/\bar{u}} - (1-y)^2 u[\Delta D_{B/d} + R\Delta D_{B/s}]}{[\bar{d}+R\bar{s}]D_{B/\bar{u}} + (1-y)^2 u[D_{B/d} + RD_{B/s}]},$$

in agreement with the results of [11].

The formulae given above hold for any baryon and antibaryon with spin 1/2. If we specify the final hadron observed, further simplifications are possible. Let us consider the case in which a Λ baryon is produced, or, in general, a baryon (rather than an antibaryon): in this case we can neglect terms which contain both $\bar{q}$ distributions (in a proton) and $\bar{q}$ fragmentations (into a Λ) as they are both small, in particular at large x and z. Then we simply have

$$P_{[\nu,\ell]}^{(\pm)}(\Lambda;z) \simeq P_{[\nu,\ell]}^{(0)}(\Lambda;z) \simeq -\frac{\Delta D_{\Lambda/u}}{D_{\Lambda/u}}, \tag{19}$$

$$P_{[\bar{\nu},\ell]}^{(\pm)}(\Lambda;z) \simeq P_{[\bar{\nu},\ell]}^{(0)}(\Lambda;z) \simeq -\frac{\Delta D_{\Lambda/d} + R\Delta D_{\Lambda/s}}{D_{\Lambda/d} + RD_{\Lambda/s}}, \tag{20}$$

and the polarizations, up to QCD evolution effects, become functions of the variable z only, since any other term apart from the fragmentation functions cancels out. For (20) to hold one should also avoid large y regions, due to the factor $(1-y)^2$ in (18).

Equations (19) and (20) relate the values of the longitudinal polarization $P(\Lambda)$ to a quantity with a clear physical meaning, i.e. the ratio $\Delta D_{\Lambda/q}/D_{\Lambda/q}$; this happens with weak charged current interactions – while it cannot happen in purely electromagnetic DIS [12] – due to the selection of the quark helicity and flavor in the coupling with neutrinos. A measurement of $P(\Lambda)$ offers new direct information on the fragmentation process. We shall discuss further this point in Sect. 5.

Similar results hold for the $\ell p \to \nu \Lambda^\uparrow X$ processes; the contributing elementary interactions are

$$\ell^- u_i \to \nu d_j,$$
$$\ell^- \bar{d}_j \to \nu \bar{u}_i,$$
$$\ell^+ d_j \to \bar{\nu} u_i,$$
$$\ell^+ \bar{u}_i \to \bar{\nu} \bar{d}_j, \tag{21}$$

with the same cross-sections as those computed in (8) and (9):

$$\frac{d\hat{\sigma}^{\ell^- u_i \to \nu d_j}}{dy} = \frac{d\hat{\sigma}^{\ell^+ \bar{u}_i \to \bar{\nu}\bar{d}_j}}{dy} = \frac{d\hat{\sigma}^{\nu d_j \to \ell^- u_i}}{dy} = \frac{d\hat{\sigma}^{\bar{\nu}\bar{d}_j \to \ell^+ \bar{u}_i}}{dy}, \tag{22}$$

$$\frac{d\hat{\sigma}^{\ell^+ d_j \to \bar{\nu}u_i}}{dy} = \frac{d\hat{\sigma}^{\ell^- \bar{d}_j \to \nu\bar{u}_i}}{dy} = \frac{d\hat{\sigma}^{\bar{\nu}u_i \to \ell^+ d_j}}{dy} = \frac{d\hat{\sigma}^{\nu\bar{u}_i \to \ell^- \bar{d}_j}}{dy}. \tag{23}$$

The analogue of (15) and (16) is now

$$P_{[\ell,\nu]}^{(\pm)}(B;x,y,z) \tag{24}$$
$$= \frac{(1-y)^2[\bar{d}_\pm + R\bar{s}_\pm]\Delta D_{B/\bar{u}} - u_\mp[\Delta D_{B/d} + R\Delta D_{B/s}]}{(1-y)^2[\bar{d}_\pm + R\bar{s}_\pm]D_{B/\bar{u}} + u_\mp[D_{B/d} + RD_{B/s}]}$$

and

$$P_{[\ell,\bar{\nu}]}^{(\pm)}(B;x,y,z) = -\Big((1-y)^2[d_\mp + Rs_\mp]\Delta D_{B/u}$$
$$-\bar{u}_\pm[\Delta D_{B/\bar{d}} + R\Delta D_{B/\bar{s}}]\Big)\Big/$$
$$\Big((1-y)^2[d_\mp + Rs_\mp]D_{B/u}$$
$$+\bar{u}_\pm[D_{B/\bar{d}} + RD_{B/\bar{s}}]\Big), \tag{25}$$

and similarly for the analogue of (17) and (18) (one simply replaces in the above equations the quark and antiquark helicity distributions with the unpolarized ones).

In the case in which one can neglect antiquark contributions (as for Λ's) one has again, as in (19) and (20),

$$P_{[\ell,\nu]}^{(\pm)}(\Lambda;z) \simeq P_{[\ell,\nu]}^{(0)}(\Lambda;z) \simeq -\frac{\Delta D_{\Lambda/d} + R\Delta D_{\Lambda/s}}{D_{\Lambda/d} + RD_{\Lambda/s}}, \tag{26}$$

$$P_{[\ell,\bar{\nu}]}^{(\pm)}(\Lambda;z) \simeq P_{[\ell,\bar{\nu}]}^{(0)}(\Lambda;z) \simeq -\frac{\Delta D_{\Lambda/u}}{D_{\Lambda/u}}. \tag{27}$$

3 Neutral current neutrino processes, $\nu p \to \nu \Lambda^\uparrow X$

There are 4 different kinds of elementary interactions contributing to these processes

$$\nu q \to \nu q,$$
$$\nu \bar{q} \to \nu \bar{q},$$
$$\bar{\nu} q \to \bar{\nu} q,$$
$$\bar{\nu} \bar{q} \to \bar{\nu} \bar{q}, \tag{28}$$

where q can be either u_j or d_j.

There are 2 non-zero independent helicity amplitudes for each process in (28). These lead, through (7), to the following elementary cross-sections

$$\frac{d\hat{\sigma}_{-+}^{\nu q \to \nu q}}{dy} = \frac{d\hat{\sigma}_{+-}^{\bar{\nu}\bar{q} \to \bar{\nu}\bar{q}}}{dy}$$
$$= \frac{\pi\alpha^2}{4xs}\frac{(2e_q\sin^2\theta_{\mathrm{W}})^2}{\sin^4\theta_{\mathrm{W}}\cos^4\theta_{\mathrm{W}}}\left(\frac{1-y}{y+M_Z^2/xs}\right)^2,$$
$$\frac{d\hat{\sigma}_{--}^{\nu q \to \nu q}}{dy} = \frac{d\hat{\sigma}_{++}^{\bar{\nu}\bar{q} \to \bar{\nu}\bar{q}}}{dy}$$
$$= \frac{\pi\alpha^2}{4xs}\frac{(1-2|e_q|\sin^2\theta_{\mathrm{W}})^2}{\sin^4\theta_{\mathrm{W}}\cos^4\theta_{\mathrm{W}}}\left(\frac{1}{y+M_Z^2/xs}\right)^2,$$

$$\frac{\mathrm{d}\hat{\sigma}^{\nu\bar{q}\to\nu\bar{q}}_{-+}}{\mathrm{d}y} = \frac{\mathrm{d}\hat{\sigma}^{\bar{\nu}q\to\bar{\nu}q}_{+-}}{\mathrm{d}y}$$

$$= \frac{\pi\alpha^2}{4xs}\frac{(1-2|e_q|\sin^2\theta_W)^2}{\sin^4\theta_W\cos^4\theta_W}\left(\frac{1-y}{y+M_Z^2/xs}\right)^2,$$

$$\frac{\mathrm{d}\hat{\sigma}^{\nu\bar{q}\to\nu\bar{q}}_{--}}{\mathrm{d}y} = \frac{\mathrm{d}\hat{\sigma}^{\bar{\nu}q\to\bar{\nu}q}_{++}}{\mathrm{d}y}$$

$$= \frac{\pi\alpha^2}{4xs}\frac{(2e_q\sin^2\theta_W)^2}{\sin^4\theta_W\cos^4\theta_W}\left(\frac{1}{y+M_Z^2/xs}\right)^2, \quad (29)$$

where e_q is the quark charge in units of the proton charge.

In analogy to what we did in the previous paragraph, the longitudinal polarization of the produced baryon B is defined by

$$P_{[\nu,\nu]}(B) = \frac{\mathrm{d}\sigma^{\nu p\to\nu B_+ X} - \mathrm{d}\sigma^{\nu p\to\nu B_- X}}{\mathrm{d}\sigma^{\nu p\to\nu B_+ X} + \mathrm{d}\sigma^{\nu p\to\nu B_- X}} \quad (30)$$

and

$$P_{[\bar{\nu},\bar{\nu}]}(B) = \frac{\mathrm{d}\sigma^{\bar{\nu} p\to\bar{\nu} B_+ X} - \mathrm{d}\sigma^{\bar{\nu} p\to\bar{\nu} B_- X}}{\mathrm{d}\sigma^{\bar{\nu} p\to\bar{\nu} B_+ X} + \mathrm{d}\sigma^{\bar{\nu} p\to\bar{\nu} B_- X}}. \quad (31)$$

For the numerator and denominator of $P_{[\nu,\nu]}(B)$ and $P_{[\bar{\nu},\bar{\nu}]}(B)$ separately, one obtains, for a generic spin state S of the proton:

$$N^{(S)}_{[\nu,\nu]}(B) \quad (32)$$
$$= \sum_j\Big\{\Big[(u_j)^{(S)}_+(1-y)^2 16C^2 - (u_j)^{(S)}_-(1-4C)^2\Big]\Delta D_{B/u_j}$$
$$+ \Big[(d_j)^{(S)}_+(1-y)^2 4C^2 - (d_j)^{(S)}_-(1-2C)^2\Big]\Delta D_{B/d_j}$$
$$+ \Big[(\bar{u}_j)^{(S)}_+(1-y)^2(1-4C)^2 - (\bar{u}_j)^{(S)}_- 16C^2\Big]\Delta D_{B/\bar{u}_j}$$
$$+ \Big[(\bar{d}_j)^{(S)}_+(1-y)^2(1-2C)^2 - (\bar{d}_j)^{(S)}_- 4C^2\Big]\Delta D_{B/\bar{d}_j}\Big\},$$

$$D^{(S)}_{[\nu,\nu]}(B) \quad (33)$$
$$= \sum_j\Big\{\Big[(u_j)^{(S)}_+(1-y)^2 16C^2 + (u_j)^{(S)}_-(1-4C)^2\Big]D_{B/u_j}$$
$$+ \Big[(d_j)^{(S)}_+(1-y)^2 4C^2 + (d_j)^{(S)}_-(1-2C)^2\Big]D_{B/d_j}$$
$$+ \Big[(\bar{u}_j)^{(S)}_+(1-y)^2(1-4C)^2 + (\bar{u}_j)^{(S)}_- 16C^2\Big]D_{B/\bar{u}_j}$$
$$+ \Big[(\bar{d}_j)^{(S)}_+(1-y)^2(1-2C)^2 + (\bar{d}_j)^{(S)}_- 4C^2\Big]D_{B/\bar{d}_j}\Big\},$$

and

$$N^{(S)}_{[\bar{\nu},\bar{\nu}]}(B) \quad (34)$$
$$= \sum_j\Big\{\Big[(u_j)^{(S)}_+ 16C^2 - (u_j)^{(S)}_-(1-y)^2(1-4C)^2\Big]\Delta D_{B/u_j}$$
$$+ \Big[(d_j)^{(S)}_+ 4C^2 - (d_j)^{(S)}_-(1-y)^2(1-2C)^2\Big]\Delta D_{B/d_j}$$
$$+ \Big[(\bar{u}_j)^{(S)}_+(1-4C)^2 - (\bar{u}_j)^{(S)}_-(1-y)^2 16C^2\Big]\Delta D_{B/\bar{u}_j}$$
$$+ \Big[(\bar{d}_j)^{(S)}_+(1-2C)^2 - (\bar{d}_j)^{(S)}_-(1-y)^2 4C^2\Big]\Delta D_{B/\bar{d}_j}\Big\},$$

$$D^{(S)}_{[\bar{\nu},\bar{\nu}]}(B) \quad (35)$$
$$= \sum_j\Big\{\Big[(u_j)^{(S)}_+ 16C^2 + (u_j)^{(S)}_-(1-y)^2(1-4C)^2\Big]D_{B/u_j}$$
$$+ \Big[(d_j)^{(S)}_+ 4C^2 + (d_j)^{(S)}_-(1-y)^2(1-2C)^2\Big]D_{B/d_j}$$
$$+ \Big[(\bar{u}_j)^{(S)}_+(1-4C)^2 + (\bar{u}_j)^{(S)}_-(1-y)^2 16C^2\Big]D_{B/\bar{u}_j}$$
$$+ \Big[(\bar{d}_j)^{(S)}_+(1-2C)^2 + (\bar{d}_j)^{(S)}_-(1-y)^2 4C^2\Big]D_{B/\bar{d}_j}\Big\},$$

where $C \equiv \sin^2\theta_W/3$.

In the case of Λ (or any baryon, rather than anti-baryon) production, a simple expression for its longitudinal polarization P can be obtained by neglecting the anti-quark contributions and the terms proportional to $\sin^4\theta_W$. For longitudinally polarized protons in this approximation we have

$$P^{(\pm)}_{[\nu,\nu]}(\Lambda) \quad (36)$$
$$\simeq -\frac{\sum_j[(u_j)_\mp(1-8C)\Delta D_{\Lambda/u_j} + (d_j)_\mp(1-4C)\Delta D_{\Lambda/d_j}]}{\sum_j[(u_j)_\mp(1-8C)D_{\Lambda/u_j} + (d_j)_\mp(1-4C)D_{\Lambda/d_j}]},$$

whereas for unpolarized proton, where $q_\pm \to q/2$, one obtains

$$P^{(0)}_{[\nu,\nu]}(\Lambda) \quad (37)$$
$$\simeq -\frac{\sum_j[u_j(1-8C)\Delta D_{\Lambda/u_j} + d_j(1-4C)\Delta D_{\Lambda/d_j}]}{\sum_j[u_j(1-8C)D_{\Lambda/u_j} + d_j(1-4C)D_{\Lambda/d_j}]}.$$

Similar formulae, avoiding the large y region, hold for $P^{(\pm)}_{[\bar{\nu},\bar{\nu}]}(\Lambda)$ and for $P^{(0)}_{[\bar{\nu},\bar{\nu}]}(\Lambda)$.

4 Neutral current lepton processes, $\ell p \to \ell\Lambda^\uparrow\ X$

The possible elementary scatterings contributing to this process are of the form

$$\ell q \to \ell q, \quad (38)$$

where ℓ can be either ℓ^+ or ℓ^- and q can be any quark or antiquark.

There are 4 non-zero independent helicity amplitudes corresponding to the process in (38). Notice that in this case we must take into account the contributions of both weak and electromagnetic interactions, and the amplitudes are given by the sum of the two corresponding terms. According to (7), the elementary cross-sections can be written as

$$\frac{\mathrm{d}\hat{\sigma}^{\ell q\to\ell q}_{\pm\pm}}{\mathrm{d}y} = \frac{\pi\alpha^2}{16xs}\left(N^{\ell q}_{\pm\pm}\frac{1}{y+M_Z^2/xs} - \frac{8e_q}{y}\right)^2, \quad (39)$$

$$\frac{\mathrm{d}\hat{\sigma}^{\ell q\to\ell q}_{\pm\mp}}{\mathrm{d}y} = \frac{\pi\alpha^2}{16xs}\left(N^{\ell q}_{\pm\mp}\frac{1}{y+M_Z^2/xs} - \frac{8e_q}{y}\right)^2(1-y)^2,$$

where again ℓ can be either ℓ^+ or ℓ^-, q can be any quark or antiquark $q = u_j, d_j$ and e_q is the quark charge. For the coefficients $N^{\ell q}$ we have ($C = \sin^2\theta_W/3$)

$$N_{++}^{\ell^- u_j} = N_{+-}^{\ell^- \bar{u}_j} = N_{-+}^{\ell^+ u_j} = N_{--}^{\ell^+ \bar{u}_j} = \frac{-16C}{1-3C} \simeq -1.60,$$

$$N_{+-}^{\ell^- u_j} = N_{++}^{\ell^- \bar{u}_j} = N_{--}^{\ell^+ u_j} = N_{-+}^{\ell^+ \bar{u}_j} = \frac{4(1-4C)}{1-3C} \simeq 3.60,$$

$$N_{-+}^{\ell^- u_j} = N_{--}^{\ell^- \bar{u}_j} = N_{++}^{\ell^+ u_j} = N_{+-}^{\ell^+ \bar{u}_j} = \frac{8(1-6C)}{3(1-3C)} \simeq 1.87,$$

$$N_{--}^{\ell^- u_j} = N_{-+}^{\ell^- \bar{u}_j} = N_{+-}^{\ell^+ u_j} = N_{++}^{\ell^+ \bar{u}_j} = \frac{2(6C-1)(1-4C)}{3C(1-3C)}$$
$$\simeq -4.19, \qquad (40)$$

and

$$N_{++}^{\ell^- d_j} = N_{+-}^{\ell^- \bar{d}_j} = N_{-+}^{\ell^+ d_j} = N_{--}^{\ell^+ \bar{d}_j} = \frac{8C}{1-3C} \simeq 0.80,$$

$$N_{+-}^{\ell^- d_j} = N_{++}^{\ell^- \bar{d}_j} = N_{--}^{\ell^+ d_j} = N_{-+}^{\ell^+ \bar{d}_j} = \frac{4(2C-1)}{1-3C} \simeq -4.40,$$

$$N_{-+}^{\ell^- d_j} = N_{--}^{\ell^- \bar{d}_j} = N_{++}^{\ell^+ d_j} = N_{+-}^{\ell^+ \bar{d}_j} = \frac{4(6C-1)}{3(1-3C)} \simeq -0.93,$$

$$N_{--}^{\ell^- d_j} = N_{-+}^{\ell^- \bar{d}_j} = N_{+-}^{\ell^+ d_j} = N_{++}^{\ell^+ \bar{d}_j} = \frac{2(1-6C)(1-2C)}{3C(1-3C)}$$
$$\simeq 5.12. \qquad (41)$$

We can now proceed to the calculation of the longitudinal polarization P of the observed spin 1/2 baryon

$$P_{[\ell,\ell]}(B) = \frac{\mathrm{d}\sigma^{\ell p \to \ell B_+ X} - \mathrm{d}\sigma^{\ell p \to \ell B_- X}}{\mathrm{d}\sigma^{\ell p \to \ell B_+ X} + \mathrm{d}\sigma^{\ell p \to \ell B_- X}}, \qquad (42)$$

where ℓ can be either ℓ^+ or ℓ^-.

$P_{[\ell,\ell]}(B)$ can be evaluated for any lepton and proton spin configuration. When both the proton p and the lepton ℓ are longitudinally polarized (in helicity states), the polarization P becomes

$$P_{[\ell,\ell]}^{(\pm,\pm)}(B) = \frac{\sum_q \left[q_\pm \mathrm{d}\hat{\sigma}_{\pm+}^{\ell q \to \ell q} - q_\mp \mathrm{d}\hat{\sigma}_{\pm-}^{\ell q \to \ell q} \right] \Delta D_{B/q}}{\sum_q \left[q_\pm \mathrm{d}\hat{\sigma}_{\pm+}^{\ell q \to \ell q} + q_\mp \mathrm{d}\hat{\sigma}_{\pm-}^{\ell q \to \ell q} \right] D_{B/q}}, \qquad (43)$$

where again ℓ stands for either ℓ^+ or ℓ^-, and the sum runs over all quarks and antiquarks, $q = u, d, s, \bar{u}, \bar{d}, \bar{s}, \cdots$

For longitudinally polarized leptons but unpolarized protons ($q_\pm \to q/2$) we have

$$P_{[\ell,\ell]}^{(\pm,0)} = \frac{\sum_q q \left[\mathrm{d}\hat{\sigma}_{\pm+}^{\ell q \to \ell q} - \mathrm{d}\hat{\sigma}_{\pm-}^{\ell q \to \ell q} \right] \Delta D_{B/q}}{\sum_q q \left[\mathrm{d}\hat{\sigma}_{\pm+}^{\ell q \to \ell q} + \mathrm{d}\hat{\sigma}_{\pm-}^{\ell q \to \ell q} \right] D_{B/q}}, \qquad (44)$$

while for unpolarized leptons but longitudinally polarized protons we have

$$P_{[\ell,\ell]}^{(0,\pm)}(B) = \left(\sum_q \left[q_\pm (\mathrm{d}\hat{\sigma}_{++}^{\ell q \to \ell q} + \mathrm{d}\hat{\sigma}_{-+}^{\ell q \to \ell q}) \right. \right.$$

$$\left. -q_\mp(\mathrm{d}\hat{\sigma}_{+-}^{\ell q \to \ell q} + \mathrm{d}\hat{\sigma}_{--}^{\ell q \to \ell q}) \right] \Delta D_{B/q} \Bigg) \Bigg/$$

$$\left(\sum_q \left[q_\pm(\mathrm{d}\hat{\sigma}_{++}^{\ell q \to \ell q} + \mathrm{d}\hat{\sigma}_{-+}^{\ell q \to \ell q}) \right. \right.$$

$$\left. \left. +q_\mp(\mathrm{d}\hat{\sigma}_{+-}^{\ell q \to \ell q} + \mathrm{d}\hat{\sigma}_{--}^{\ell q \to \ell q}) \right] D_{B/q} \right). \qquad (45)$$

Finally, the most interesting case is when neither the proton nor the lepton are polarized: in this case the longitudinal polarization of baryon B is non-zero only due to parity violating weak contributions. We obtain

$$P_{[\ell,\ell]}^{(0,0)}(B) = \left(\sum_q q \left[\mathrm{d}\hat{\sigma}_{++}^{\ell q \to \ell q} + \mathrm{d}\hat{\sigma}_{-+}^{\ell q \to \ell q} \right. \right.$$

$$\left. \left. -\mathrm{d}\hat{\sigma}_{+-}^{\ell q \to \ell q} - \mathrm{d}\hat{\sigma}_{--}^{\ell q \to \ell q} \right] \Delta D_{B/q} \right) \Bigg/$$

$$\left(4 \sum_q q \mathrm{d}\hat{\sigma}^{\ell q \to \ell q} D_{B/q} \right), \qquad (46)$$

where $\mathrm{d}\hat{\sigma}^{\ell q \to \ell q}$ is the unpolarized $\ell q \to \ell q$ cross-section

$$4\mathrm{d}\hat{\sigma}^{\ell q \to \ell q} = \mathrm{d}\hat{\sigma}_{++}^{\ell q \to \ell q} + \mathrm{d}\hat{\sigma}_{-+}^{\ell q \to \ell q} + \mathrm{d}\hat{\sigma}_{+-}^{\ell q \to \ell q} + \mathrm{d}\hat{\sigma}_{--}^{\ell q \to \ell q}. \quad (47)$$

This effect might be measurable at HERA and numerical estimates will be given in the next section.

5 Numerical estimates

In the previous sections we have obtained explicit expressions for the polarization of baryons produced in DIS scatterings involving weak interactions; we now use these formulae to give predictions in the case of Λ and $\bar{\Lambda}$ production, considering typical kinematical configurations of ongoing or planned experiments. When convenient, we integrate over the actual physical ranges of some variables; these are collected in Table 1 of Appendix A. Our results should give a good comprehensive description of what to expect in all present or future experiments, and can be adapted to cover all realistic situations, according to different kinematical cuts and configurations.

The polarization values depend on the known standard model dynamics, on the rather well known partonic distributions, both unpolarized and polarized, and on the quark fragmentation functions, again both unpolarized and polarized. The latter are not so well known and a choice must be made in order to give numerical estimates or in order to be able to interpret the measured values in favor of a particular set.

Unpolarized Λ fragmentation functions are determined by fitting $e^+ e^- \to \Lambda + \bar{\Lambda} + X$ experimental data, which are sensitive only to singlet combinations, like $D_{\Lambda/q} + D_{\Lambda/\bar{q}} \equiv D_{(\Lambda+\bar{\Lambda})/q}$. It is impossible to separate the fragmentation functions relative to Λ's from those for $\bar{\Lambda}$'s in a model independent way; also flavor separation is not possible without appropriate initial assumptions, for example about

$SU(3)$ flavor symmetry. Polarized Λ fragmentation functions are obtained by fitting the scarce data on Λ polarization at LEP, sensitive only to non-singlet combinations like $\Delta D_{\Lambda/q} - \Delta D_{\Lambda/\bar{q}} = \Delta D_{\Lambda/q}^{\text{val}}$. Also in this case flavor separation has to rely on models.

Three typical sets of fragmentation functions, denoted as scenarios 1, 2 and 3, and derived from fits to e^+e^- data, are given in [4]. The unpolarized fragmentation functions are taken to be $SU(3)$ symmetric:

$$D_{(\Lambda+\bar{\Lambda})/u} = D_{(\Lambda+\bar{\Lambda})/d} = D_{(\Lambda+\bar{\Lambda})/s} = D_{(\Lambda+\bar{\Lambda})/\bar{u}}$$
$$= D_{(\Lambda+\bar{\Lambda})/\bar{d}} = D_{(\Lambda+\bar{\Lambda})/\bar{s}}, \qquad (48)$$

and have been derived for the combined production of Λ and $\bar{\Lambda}$ and not for each of them separately.

For the polarized fragmentation functions they assume, at the initial scale μ^2,

$$\Delta D_{\Lambda/s}(z, \mu^2) = z^\alpha D_{(\Lambda+\bar{\Lambda})/s}(z, \mu^2), \qquad (49)$$
$$\Delta D_{\Lambda/u}(z, \mu^2) = \Delta D_{\Lambda/d}(z, \mu^2) = N_u \Delta D_{\Lambda/s}(z, \mu^2).$$

The three scenarios differ for the relative contributions of the strange quark polarization to Λ polarization: $N_u = 0$, $N_u = -0.2$ and $N_u = 1$ for scenarios 1, 2 and 3 respectively [4]. The "unfavored" polarized fragmentations $\Delta D_{\Lambda/\bar{u}}, \Delta D_{\bar{\Lambda}/u}$, etc. are assumed to be negligible at the initial scale μ^2, and are only generated by QCD evolution; it is then possible, for the polarized fragmentation functions, to obtain separately the contributions to Λ and $\bar{\Lambda}$.

We adopt the above set of fragmentation functions as they are the least dependent on models, they have the proper QCD evolution, and the three scenarios are well representative of possible spin dependences. We are then equipped with unpolarized fragmentation functions into $\Lambda + \bar{\Lambda}$ and with separate polarized fragmentation functions into Λ and $\bar{\Lambda}$; we wish to give predictions and estimates for the polarizations of Λ and $\bar{\Lambda}$, which are measured separately. We then define the following computable quantities:

$$P^*(\Lambda) \equiv \frac{d\sigma^{\Lambda_+} - d\sigma^{\Lambda_-}}{d\sigma^{\Lambda+\bar{\Lambda}}} = \frac{P(\Lambda)}{1+T}, \qquad (50)$$

and

$$P^*(\bar{\Lambda}) \equiv \frac{d\sigma^{\bar{\Lambda}_+} - d\sigma^{\bar{\Lambda}_-}}{d\sigma^{\Lambda+\bar{\Lambda}}} = P(\bar{\Lambda}) \frac{T}{1+T}, \qquad (51)$$

where the notations should be obvious and

$$T = \frac{d\sigma^{\bar{\Lambda}}}{d\sigma^{\Lambda}}. \qquad (52)$$

Equations (50) and (51) allow us to compute the values of $P(\Lambda)$ and $P(\bar{\Lambda})$ provided one can compute or measure the ratio T:

$$P(\Lambda) = (1+T)P^*(\Lambda), \quad P(\bar{\Lambda}) = \left(1 + \frac{1}{T}\right)P^*(\bar{\Lambda}). \qquad (53)$$

Notice that P is always larger in magnitude than P^*.

The ratio T cannot be computed with the fragmentation set of [4]; it requires the knowledge of separate unpolarized fragmentation functions for Λ and $\bar{\Lambda}$ and it depends on the chosen set.

In Figs. 1–10 we show some results for $P^*(\Lambda, \bar{\Lambda})$ for several processes, with different initial spin configurations, and different kinematical conditions, corresponding to typical experimental setups, shown in Table 1 of Appendix A. These may easily be changed, according to experimental situations. Details are given in the figure captions. We use the unpolarized distribution functions of [14], the related polarized distribution functions of [15] (we have explicitly checked that our numerical results depend very little on the available sets of parton densities) and the fragmentation functions of [4], mainly with scenarios 2 and 3.

In Figs. 11 and 12 we give estimates for $P(\Lambda)$ [rather than $P^*(\Lambda)$], in the same cases as some of the previous figures; we have computed the ratio T either with the $SU(3)$ symmetric set of unpolarized fragmentation functions of [9] or with a set derived from [16], by imposing $SU(3)$ symmetry.

The figure captions contain all relevant information about the various cases; we give here some general comments about our results.

(1) We present results using mainly the fragmentation functions of scenarios 2 and 3 of [4], neglecting scenario 1, in which only s quarks contribute to the Λ polarization. In fact, $P(\Lambda)$ is always negligible in this case, given the small content of s quarks in the nucleon target and the $SU(3)$-symmetric nature of the unpolarized fragmentation functions utilized. This can be seen by inspecting (19), (20) and (26), (27) for charged current interactions and (37) for neutral currents. However, it is interesting to notice that for unpolarized fragmentation functions allowing for a strong $SU(3)$ symmetry breaking, like those of [16], the situation can be different, and scenario 1 might give sizable asymmetries. According to [16], $D_{\Lambda/u} = D_{\Lambda/d} \ll D_{\Lambda/s}$ and this can well compensate for the small factor R in (20), so that, also in scenario 1, $P_{[\bar{\nu},\ell]}$ can be large.

(2) Figures 1, 2 and 11 summarize some of the most interesting features of Λ polarization in charged current interactions. The large $\langle x \rangle$ values involved in the NOMAD experiment imply $T = d\sigma^{\bar{\Lambda}}/d\sigma^{\Lambda} \ll 1$, so that, from (50), $P^*(\Lambda)$ is similar to $P(\Lambda)$ (compare Figs. 2 and 11) and follows closely the simple behavior suggested by (19) and (20). $P^*(\bar{\Lambda})$, instead, is suppressed by the small ratio T, see (51); the actual estimated value of $P(\bar{\Lambda})$ is shown in Fig. 11 and is much larger. Notice that a comparison between Figs. 1 and 2, i.e. between (19) and (20), might give information on the ratios $C_q \equiv \Delta D_{\Lambda/q}/D_{\Lambda/q}$; for example, the same value of C_q for all flavors would result in $P_{[\nu,\ell]}(\Lambda) = P_{[\bar{\nu},\ell]}(\Lambda)$. On the other hand, largely different values of $P_{[\nu,\ell]}$ and $P_{[\bar{\nu},\ell]}$ would certainly indicate a strong $SU(3)$ symmetry breaking in the fragmentation functions, with s quark contributions dominating in order to compensate for the small R factor in (20).

Some data on $P_{[\nu,\ell]}^{(0)}(\Lambda, \bar{\Lambda})$ are available from the NOMAD collaboration [13], but the errors and uncertainties
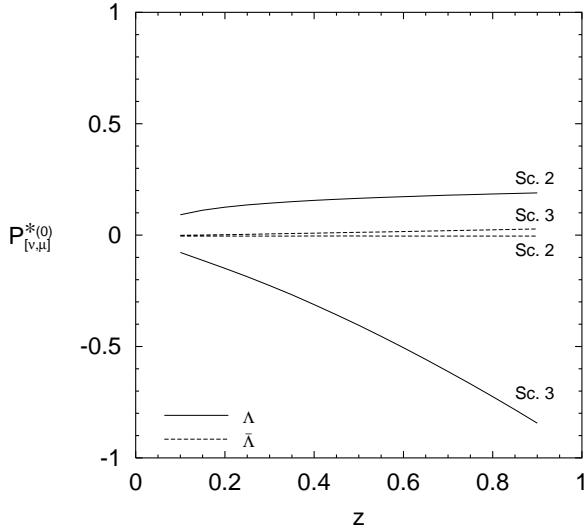
Fig. 1. $P^{*(0)}_{[\nu,\mu]}$ for Λ (solid lines) and $\bar{\Lambda}$ (dashed lines) hyperons, as a function of z, with a kinematical setup typical for the NOMAD experiment at CERN (see Table 1 for details). Results are given for scenarios 2 and 3 of the polarized Λ fragmentation functions (FF) of [4]. Results with scenario 1 are almost negligible. Unpolarized $(\Lambda + \bar{\Lambda})$ FF are from [4]; unpolarized GRV [14] partonic distributions have been used for the proton target. Since $\langle x \rangle$ is large for this kinematical configuration, we expect $T = \mathrm{d}\sigma^{\bar{\Lambda}}/\mathrm{d}\sigma^{\Lambda} \ll 1$ and, as a consequence, $P^{(0)}_{[\nu,\mu]}(\Lambda) \simeq P^{*(0)}_{[\nu,\mu]}(\Lambda)$, while $P^{(0)}_{[\nu,\mu]}(\bar{\Lambda}) \gg P^{*(0)}_{[\nu,\mu]}(\bar{\Lambda})$ (see text for more details)

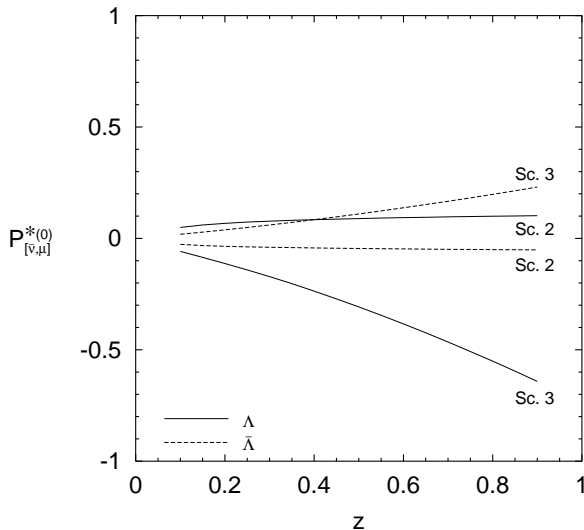**Fig. 2.** $P^{*(0)}_{[\bar{\nu},\mu]}$ for Λ (solid lines) and $\bar{\Lambda}$ (dashed lines) hyperons, as a function of z, with a kinematical setup typical for the NOMAD experiment at CERN (see Table 1 for details). Results are given for scenarios 2 and 3 of the polarized Λ FF of [4]. Results with scenario 1 are almost negligible. Unpolarized $(\Lambda + \bar{\Lambda})$ FF are from [4]; unpolarized GRV [14] partonic distributions have been used for the proton target. Since $\langle x \rangle$ is large for this kinematical configuration, we expect $T = \mathrm{d}\sigma^{\bar{\Lambda}}/\mathrm{d}\sigma^{\Lambda} \ll 1$ and, as a consequence, $P^{(0)}_{[\bar{\nu},\mu]}(\Lambda) \simeq P^{*(0)}_{[\bar{\nu},\mu]}(\Lambda)$, while $P^{(0)}_{[\bar{\nu},\mu]}(\bar{\Lambda}) \gg P^{*(0)}_{[\bar{\nu},\mu]}(\bar{\Lambda})$ (see text and Fig. 11 for more details)
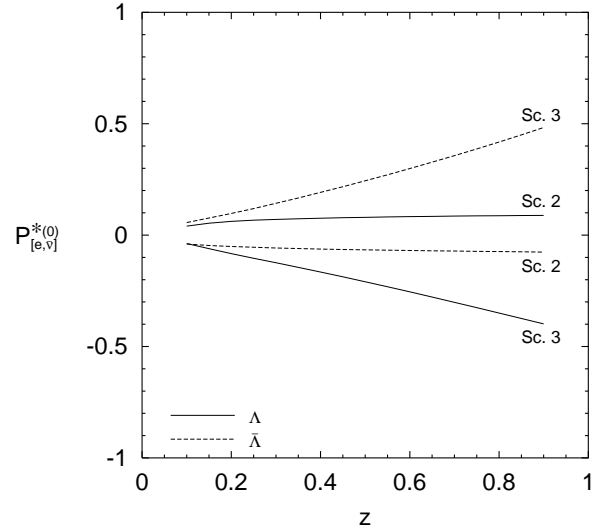

Fig. 3. $P^{*(0)}_{[e,\bar{\nu}]}$ for Λ (solid lines) and $\bar{\Lambda}$ (dashed lines) hyperons, as a function of z, with a kinematical setup typical for the HERA experiments at DESY (see Table 1 for details). Results are given for scenarios 2 and 3 of the polarized Λ FF of [4]. Results with scenario 1 are almost negligible. Unpolarized $(\Lambda + \bar{\Lambda})$ FF are from [4]; unpolarized GRV [14] partonic distributions have been used for the proton target. Since $\langle x \rangle$ is small for the HERA kinematical configurations, we expect $T = \mathrm{d}\sigma^{\bar{\Lambda}}/\mathrm{d}\sigma^{\Lambda} \simeq 1$ and, as a consequence, $P^{(0)}_{[e,\bar{\nu}]}(\Lambda, \bar{\Lambda}) \simeq 2P^{*(0)}_{[e,\bar{\nu}]}(\Lambda, \bar{\Lambda})$ (see text for more details)

are still too large to allow for significant comparisons and to discriminate between different sets of fragmentation functions.

(3) Figure 3 gives values of $P^*(\Lambda)$ in kinematical regions dominated by small x values, so that one expects $T \simeq 1$ and $P^*(\Lambda, \bar{\Lambda}) \simeq P(\Lambda, \bar{\Lambda})/2$, see (50) and (51). The opposite signs of $P(\Lambda)$ and $P(\bar{\Lambda})$ can be easily understood by looking at (25) (with $q_\pm \to q/2$) and noticing that fragmentation into a baryon or an antibaryon favors the first or the second term in the numerator.

(4) For neutrino charged currents we give numerical estimates only in the case of an unpolarized target. In fact, present intensities of neutrino beams require very large targets to reach reasonable luminosities and statistics, and this makes it unpractical to polarize them. There are however proposals for neutrino factories with large intensities which will allow one to consider the option of polarized targets [17].

(5) The Λ polarizations for neutral currents shown in Figs. 4–7 exhibit a similar behavior for the four different kinematical setups considered. The differences are related to the different kinematical cuts and again to the value of the factor T. In particular, since $T \simeq 1$ for the E665 and HERA kinematics, the P^* are suppressed by a factor $\simeq 2$ with respect to the case of HERMES and COMPASS kinematics. Notice also that in these two cases there are sizable variations depending on the different polarization states of the target.

(6) The results presented in Figs. 8 and 12 show polarizations as functions of x (integrated over z) rather than z
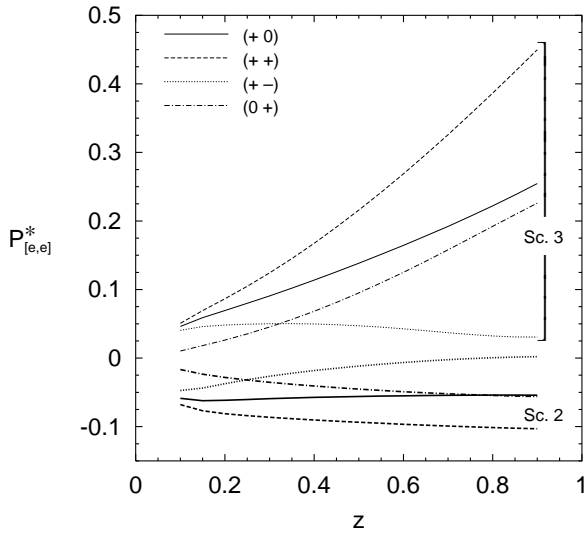
Fig. 4. $P_{[e,e]}^*$ for Λ hyperons, as a function of z, for different combinations of the beam and target polarizations, as shown in the plot legend. The kinematical setup is typical for the HERMES experiment at DESY (see Table 1 for details). Results are given for scenarios 2 (heavy lines) and 3 (thin lines) of the polarized Λ FF of [4]. Results with scenario 1 are almost negligible. Unpolarized $(\Lambda + \bar{\Lambda})$ FF are from [4]; unpolarized GRV [14] and polarized GRSV-ST [15] partonic distributions have been used for the proton target. Since $\langle x \rangle$ is large for the HERMES kinematical configuration, we expect, at large z, $T = d\sigma^{\bar{\Lambda}}/d\sigma^{\Lambda} \ll 1$ and, as a consequence, $P_{[e,e]}(\Lambda) \simeq P_{[e,e]}^*(\Lambda)$, while for the $\bar{\Lambda}$ (not shown in this plot) there should result $P_{[e,e]}(\bar{\Lambda}) \gg P_{[e,e]}^*(\bar{\Lambda})$ (see text for more details)

Fig. 5. $P_{[\mu,\mu]}^*$ for Λ hyperons, as a function of z, for different combinations of the beam and target polarizations, as shown in the plot legend. The kinematical setup is typical for the COMPASS experiment at CERN (see Table 1 for details). Results are given for scenarios 2 (heavy lines) and 3 (thin lines) of the polarized Λ FF of [4]. Results with scenario 1 are almost negligible. Unpolarized $(\Lambda + \bar{\Lambda})$ FF are from [4]; unpolarized GRV [14] and polarized GRSV-ST [15] partonic distributions have been used for the proton target. Since $\langle x \rangle$ is relatively large for the COMPASS kinematical configuration, we expect, at large z, $T = d\sigma^{\bar{\Lambda}}/d\sigma^{\Lambda} \ll 1$ and, as a consequence, $P_{[\mu,\mu]}(\Lambda) \simeq P_{[\mu,\mu]}^*(\Lambda)$, while for the $\bar{\Lambda}$ (not shown in this plot) there should result $P_{[\mu,\mu]}(\bar{\Lambda}) \gg P_{[\mu,\mu]}^*(\bar{\Lambda})$ (see text for more details)

(integrated over x): these test the dynamics of the partonic process and in particular the contribution of electro-weak interferences, in a neat and unusual way. The differences between positively and negatively charged leptons are entirely due to electro-weak effects; this is well visible at large x (implying large Q^2), where the curves for e^+ and e^- differ sizably. Moreover, from (39)–(41) it is possible to evaluate analytically the zeros of the cross-section differences $d\hat{\sigma}_{\pm+} - d\hat{\sigma}_{\pm-}$ appearing in the numerator of (44); one can show that real zeros for $0 < x < 1$ occur only for electromagnetic + weak contributions and for positron beams. The effective position of the zeros depends on y (or alternatively on Q^2) and for the dominating small y values is around $x \simeq 0.04$–0.08. Although the statistical errors increase sizably for large x values at HERA, the different behavior shown at small and large x values for positron and electron beams might probably be tested.

Figure 12 shows the same plots as in Fig. 8, for the actual polarization $P(\Lambda)$, estimated according to the comments in the figure caption, rather than for $P^*(\Lambda)$; it is interesting to note how the differences between P and P^* vary with x, according to the observations we have already made.

(7) Figure 9 shows the parity violating longitudinal polarization of Λ's produced from unpolarized initial electrons and nucleons in NC processes; being a purely electro-weak effect it is more sizable at very large Q^2 values, which are,
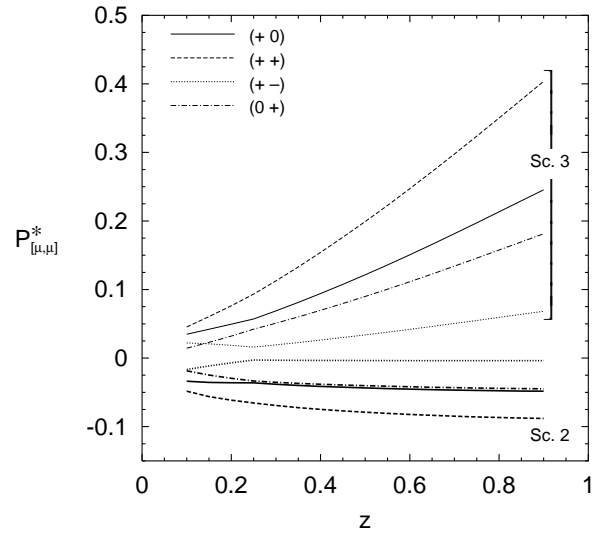
however, accessible at HERA. Also Fig. 10 shows some effects of electro-weak interferences, resulting in differences between plots of $P_{[e,e]}^{*(+,0)}$ for positrons and electrons.

We have given a comprehensive discussion – both theoretical (at LO) and phenomenological – of the polarization of Λ's and $\bar{\Lambda}$'s produced in the current fragmentation region of DIS processes, both with neutral and charged currents. Our results can be exploited to gather new information about polarized fragmentation functions, to improve our knowledge about polarized parton densities [18] and to test fundamental features of electro-weak elementary interactions. Several experiments are either running or being planned, which will precisely look at these semi-inclusive DIS processes; our study should help in the analysis of the forthcoming data.
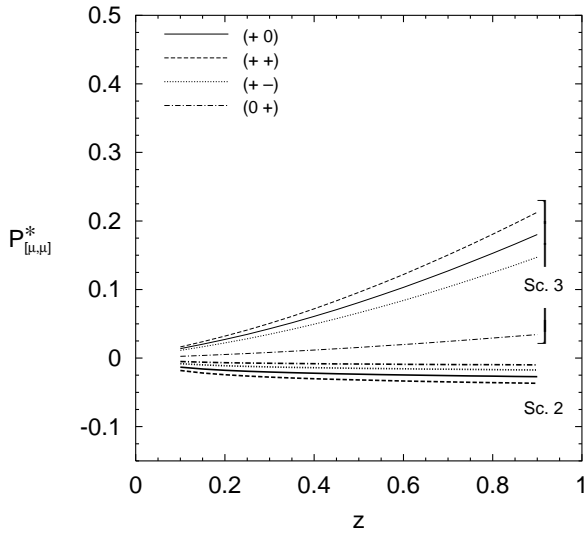
Fig. 6. $P^*_{[\mu,\mu]}$ for Λ hyperons, as a function of z, for different combinations of the beam and target polarizations, as shown in the plot legend. The kinematical setup is typical for the E665 experiment at SLAC (see Table 1 for details). Results are given for scenarios 2 (heavy lines) and 3 (thin lines) of the polarized Λ FF of [4]. Results with scenario 1 are almost negligible. Unpolarized $(\Lambda + \bar{\Lambda})$ FF are from [4]; unpolarized GRV [14] and polarized GRSV-ST [15] partonic distributions have been used for the proton target. Since $\langle x \rangle$ is relatively small for the E665 kinematical configuration, we expect $T = \mathrm{d}\sigma^{\bar{\Lambda}}/\mathrm{d}\sigma^{\Lambda} \simeq 1$ and, as a consequence, $P_{[\mu,\mu]}(\Lambda, \bar{\Lambda}) \simeq 2P^*_{[\mu,\mu]}(\Lambda, \bar{\Lambda})$ (see text for more details)

Fig. 7. $P^*_{[e,e]}$ for Λ hyperons, as a function of z, for different combinations of the positron beam and target polarizations, as shown in the plot legend. The kinematical setup is typical for the HERA experiments at DESY (see Table 1 for details). Results are given for scenarios 2 (heavy lines) and 3 (thin lines) of the polarized Λ FF of [4]. Results with scenario 1 are almost negligible. Unpolarized $(\Lambda + \bar{\Lambda})$ FF are also from [4]; unpolarized GRV [14] and polarized GRSV-ST [15] partonic distributions have been used for the proton target. Since $\langle x \rangle$ is small for the HERA kinematical configurations, we expect $T = \mathrm{d}\sigma^{\bar{\Lambda}}/\mathrm{d}\sigma^{\Lambda} \simeq 1$ and, as a consequence, $P_{[e,e]}(\Lambda, \bar{\Lambda}) \simeq 2P^*_{[e,e]}(\Lambda, \bar{\Lambda})$ (see text for more details)

Appendix

A Experimental setups and kinematical cuts

In our analysis we have considered most present and forthcoming experiments, which cover many different kinematical configurations. For the reader's convenience, we collect and summarize here the corresponding experimental setups, with their kinematical ranges.

The main variables which specify the various setups are listed below, while the kinematical values and cuts for the different experiments are given in Table 1. We use the following notation: E_l is the incoming lepton energy, in the laboratory reference frame; $\sqrt{s}$ the total energy, in the lepton–proton c.m. frame; W is the total energy, in the virtual boson–proton c.m frame; $E_{l'}$ is the outgoing lepton energy, in the laboratory frame; $\theta_{l'(h)}$ the outgoing lepton (hadron) scattering angle, in the laboratory frame; E_h is the outgoing hadron energy, in the laboratory frame; p_{T} denotes the transverse hadron momentum (with respect to the lepton direction); and $\eta = -\ln\tan(\theta_h/2)$ is the pseudorapidity, in the laboratory frame. $x = Q^2/2q \cdot p$, $y = q \cdot p/\ell \cdot p$, $z = p_h \cdot p/q \cdot p$ are the usual invariant variables for semi-inclusive DIS hadron production.

Wherever possible we have considered kinematical cuts identical to those already adopted or planned for the related experiments; the Q^2 range for the E665 experiment at SLAC $(0.25 < Q^2 < 2.5 \, \mathrm{GeV}^2)$ reaches too low Q^2
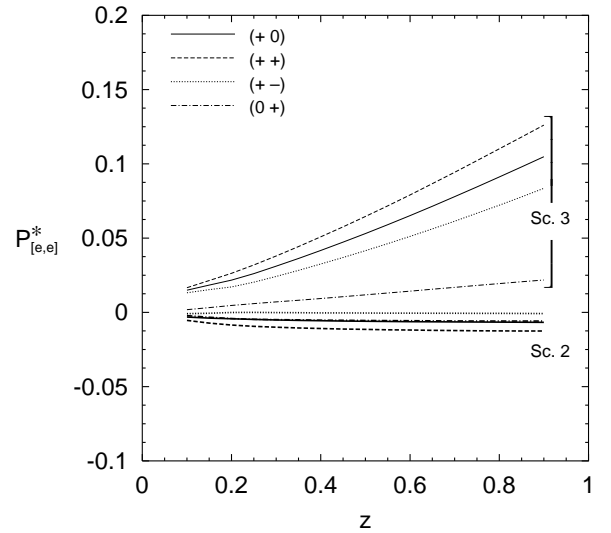
values for our leading order analysis, based on factorization theorem, and we have adopted the range $1.0 < Q^2 < 2.5 \, \mathrm{GeV}^2$ (this influences also the lower cut on x, of course).

Notice also that with HERA we mean both H1 and ZEUS typical setups at intermediate Q^2 values, while with HERA* we refer to setups with very high Q^2 values, as required for the study of electro-weak interference effects.

For the NOMAD experiment, all kinematical variables are fixed to the corresponding average value [19].

B Mass correction effects

In this paper fragmentation functions are always expressed as a function of $z = p \cdot p_h/p \cdot q$, where p, p_h, q are the four-momenta of the target proton, the produced hadron, and the virtual boson respectively. In the case of semi-inclusive DIS, at LO and in collinear configuration, z coincides with the light-cone momentum fraction of the parent parton carried by the observed hadron, $\xi = p_h^+/p_q^+$. There are in general several other variables that can be considered; depending on the specific process under study, they can be more or less suitable than z to, e.g., describe the process from the experimental point of view or to show scaling properties of observables, like cross-sections. In this appendix, we briefly review the definition of these variables and give their mutual connection. It is important to no-

Table 1. Summary of the experiments and the corresponding kinematical setups

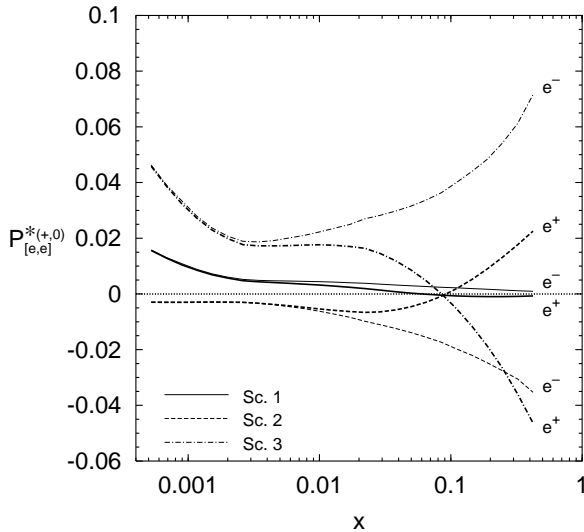|	HERMES	COMPASS	E665	NOMAD	HERA	HERA*
E_l [GeV]	27.6	200	470	48.8	27.6	27.6
$\sqrt{s}$ [GeV]	7.26	19.4	29.7	9.6	300	300
x	0.023–08	> 0.01	(10^{-3})–0.1	0.22	> 0.004	> 0.01
y	< 0.85	0.1–0.9	0.1–0.8	0.48	0.04–0.95	0.1–0.95
z	0.2–0.7	0.2–0.9	0.1–0.95		> 0.1	> 0.1
Q^2 [GeV^2]	1–24	> 4	(1)–2.5	9	10–2000	200–10^4
W [GeV]	> 2			5.8		
$E_{l'}$ [GeV]	> 4.1		< 420		> 10	> 10
$\theta_{l'}$ [rad]	0.04–0.22					
E_h [GeV]	> 2	> 5	> 4			
p_T [GeV]					> 0.5	
η					-1.5–1.5	

Fig. 8. $P^{*(+,0)}_{[e,e]}$ for Λ hyperons, as a function of x, both for positron (heavy lines) and electron (thin lines) beams. The kinematical setup is typical for the HERA experiments at DESY (see Table 1 for details). Results are given for all the three scenarios of the polarized Λ FF of [4]. Unpolarized $(\Lambda + \bar{\Lambda})$ FF are from [4]; unpolarized GRV [14] partonic distributions have been used for the proton target. The crossing at $x \simeq 0.1$ for the case of the positron beam is due to the interference between electromagnetic and weak contributions. Since $T = \mathrm{d}\sigma^{\bar{\Lambda}}/\mathrm{d}\sigma^{\Lambda}$ is $\ll 1$ at large x and becomes comparable to unity at very low x, we expect, correspondingly, $P_{[e,e]}(\Lambda) \simeq P^*_{[e,e]}(\Lambda)$ and $P_{[e,e]}(\Lambda, \bar{\Lambda}) \simeq 2P^*_{[e,e]}(\Lambda, \bar{\Lambda})$ (see text and Fig. 12 for more details)

Fig. 9. $P^{*(0,0)}_{[e,e]}$ for Λ hyperons, as a function of z, for various "high-Q^2" options of the HERA kinematical setup (see the HERA* setup in Table 1 for details) and for a positron beam: $y > 0.1$ (solid lines); $y > 0.6$ (dashed lines); $Q^2 > 4000\,\mathrm{GeV}^2$ (dot-dashed lines). Results are given for scenarios 2 (heavy lines) and 3 (thin lines) of the polarized Λ FF of [4]. Results with scenario 1 are almost negligible. Unpolarized $(\Lambda + \bar{\Lambda})$ FF are from [4]; unpolarized GRV [14] partonic distributions have been used for the proton target (see text for more details)

tice that at very large energy scales E, when the mass of the observed hadron M_h can be safely neglected, all these variables coincide (excluding the regions where they are comparable to M_h/E). However, the kinematics for most of the running or forthcoming experiments on semi-inclusive hadron production, which is the main subject of this paper, are such that mass corrections can be relevant.
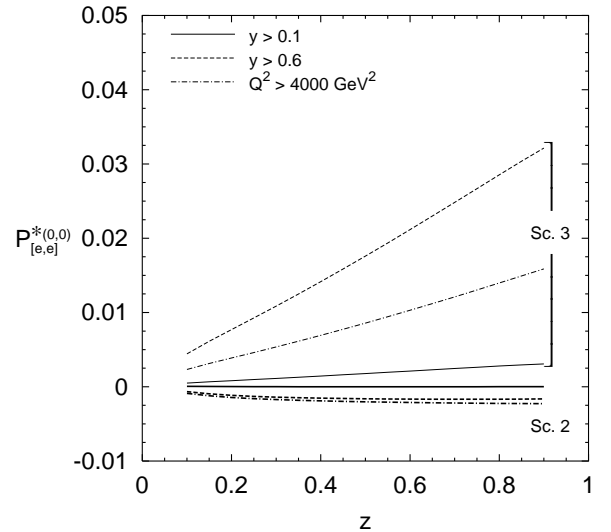
We always neglect corrections due to the mass of the proton target, even though they might have some effects in particular kinematical ranges.

Let us first briefly summarize the situation in the case of the $e^+e^- \to \Lambda X$ process, which is used to fix the set of $\Lambda + \bar{\Lambda}$ fragmentation functions largely adopted in this paper. The variables usually utilized are

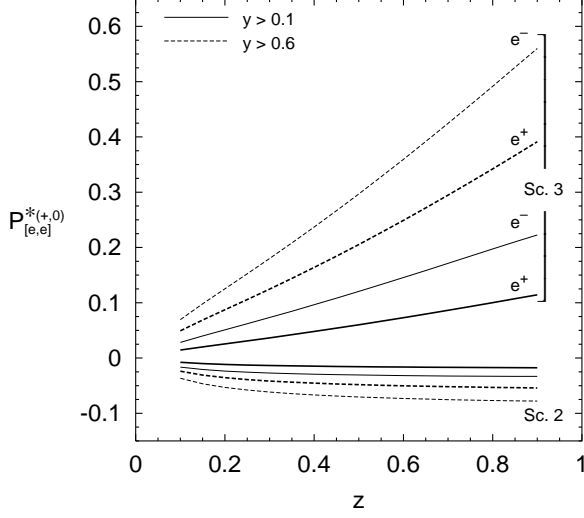$$x_E = \frac{2p_h \cdot q}{Q^2} = \frac{2E_h}{\sqrt{s}},$$

Fig. 10. $P_{[e,e]}^{*(+,0)}$ for Λ hyperons, as a function of z, both for positron (heavy lines) and electron (thin lines) beams, and for various "high-Q^2" options of the HERA kinematical setup (see the HERA* setup in Table 1 for details): $y > 0.1$ (solid lines); $y > 0.6$ (dashed lines). Results are given for scenarios 2 and 3 of the polarized Λ FF of [4]. Results with scenario 1 are almost negligible. Unpolarized $(\Lambda + \bar{\Lambda})$ FF are from [4]; unpolarized GRV [14] partonic distributions have been used for the proton target (see text for more details)

$$x_p = \frac{2|\boldsymbol{p}_h|}{Q} = \frac{2|\boldsymbol{p}_h|}{\sqrt{s}}, \tag{54}$$
$$\xi = \frac{p_h^+}{p_q^+},$$

where $\boldsymbol{p}_h$ is the hadron three-momentum in the e^+e^- c.m. reference frame. x_E and x_p are usually adopted by the experimentalists, while ξ is more commonly used by the theorists. At large energies, like in e^+e^- collisions at the Z_0 pole, and considering $x_E > 0.1$, which is also required for other theoretical reasons, see [4], mass effects are in fact negligible and all these variables can be safely assumed to be equivalent; the fragmentation function dependence on ξ can then be directly identified with the x_E dependence shown by the experimental results. When mass corrections are relevant, the connection of the variables defined in (54) is given, at leading order, by the following:

$$x_p = x_E \beta,$$
$$\xi = x_E \frac{1+\beta}{2}, \tag{55}$$

where the factor β is defined as

$$\beta = \left(1 - \frac{4M_h^2}{x_E^2 s}\right)^{1/2}. \tag{56}$$

Let us now consider the case of semi-inclusive DIS, in the virtual boson-target proton c.m. reference frame, for hadron production in the current fragmentation region
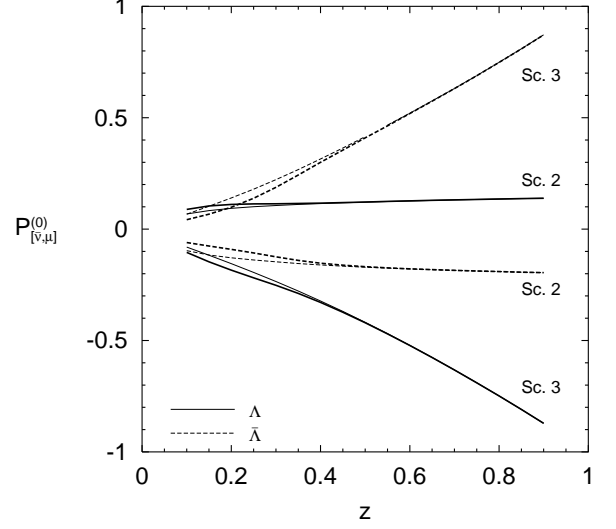

Fig. 11. $P_{[\bar{\nu},\mu]}^{(0)}$ for Λ (solid lines) and $\bar{\Lambda}$ (dashed lines) hyperons, as a function of z, with a kinematical setup typical for the NOMAD experiment at CERN (see Table 1 for details). Results are given for scenarios 2 and 3 of the polarized Λ FF of [4]. Results with scenario 1 are almost negligible. Unpolarized $(\Lambda + \bar{\Lambda})$ FF are from [4]; unpolarized GRV [14] partonic distributions have been used for the proton target. Estimates for $P_{[\bar{\nu},\mu]}^{(0)}$ are obtained from (53) by using the corresponding results for $P_{[\bar{\nu},\mu]}^{*(0)}$, shown in Fig. 2, and evaluating $T = d\sigma^{\bar{\Lambda}}/d\sigma^{\Lambda}$ with the Λ, $\bar{\Lambda}$ unpolarized FF of [9] (heavy lines) and [16] (thin lines); this last set has been modified by imposing $SU(3)$ symmetry. The spread between the two corresponding sets of curves gives a good indication of the uncertainty due to the evaluation of the ratio T. Notice that this uncertainty is almost negligible for large z, where polarizations are expected to be sizable for both scenarios 2 and 3

($x_{\mathrm{F}} > 0$). The usual variables are

$$z = \frac{p \cdot p_h}{p \cdot q} = \frac{E_h + |\boldsymbol{p}_h|}{W},$$
$$x_{\mathrm{F}} = \frac{2p_{\mathrm{L}}}{W} = \frac{2|\boldsymbol{p}_h|}{W}, \tag{57}$$
$$z' = \frac{E_h}{E_{q'}} = \frac{E_h}{(1-x)E_p} = \frac{2E_h}{W},$$

where $E_{q'}$ is the energy of the parent quark in the process $q' \to h + X$. x_{F} and z are the variables usually adopted by the experimentalists. However, as shown in [4], the appropriate scaling variable for semi-inclusive DIS is z' rather than x_{F}.

Defining $\epsilon = M_h/W$, the ranges of variation of the three variables are

$$x_{\mathrm{F}} \in \left[0, \left(1 - 4\epsilon^2\right)^{1/2}\right],$$
$$z' \in [2\epsilon, 1], \tag{58}$$
$$z \in \left[\epsilon, \frac{1}{2}\{1 + \left(1 - 4\epsilon^2\right)^{1/2}\}\right].$$
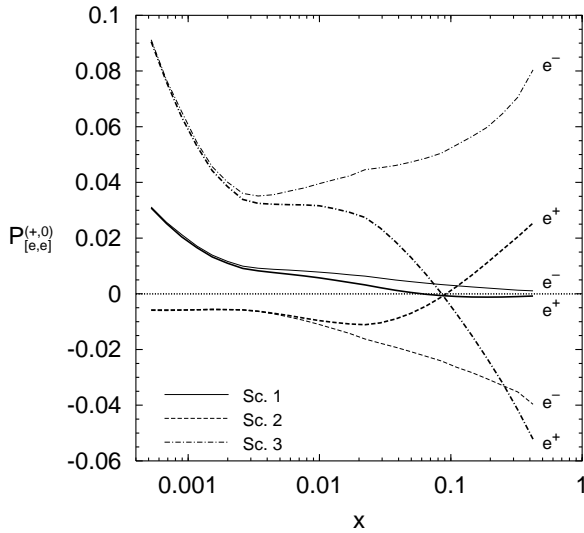
Fig. 12. $P_{[e,e]}^{(+,0)}$ for Λ hyperons, as a function of x, both for positron (heavy lines) and electron (thin lines) beams. The kinematical setup is typical for the HERA experiments at DESY (see Table 1 for details). Results are given for all the three scenarios of the polarized Λ FF of [4]. Unpolarized $(\Lambda + \bar{\Lambda})$ FF are from [4]; unpolarized GRV [14] partonic distributions have been used for the proton target. Estimates for $P_{[e,e]}^{(+,0)}$ are obtained from (53) by using the corresponding results for $P_{[e,e]}^{*(+,0)}$, shown in Fig. 8, and evaluating $T = \mathrm{d}\sigma^{\bar{\Lambda}}/\mathrm{d}\sigma^{\Lambda}$ with the Λ unpolarized FF of [9]. The crossing at $x \simeq 0.1$ for the case of positron beam is due to the interference between electromagnetic and weak contributions. Since $T = \mathrm{d}\sigma^{\bar{\Lambda}}/\mathrm{d}\sigma^{\Lambda}$ is $\ll 1$ at large x and becomes comparable to unity at very low x, we find, correspondingly, $P_{[e,e]}(\Lambda) \simeq P_{[e,e]}^{*}(\Lambda)$ and $P_{[e,e]}(\Lambda, \bar{\Lambda}) \simeq 2P_{[e,e]}^{*}(\Lambda, \bar{\Lambda})$ (see text and Fig. 8 for more details)

The expressions of the three variables as a function of the other two are

$$x_{\mathrm{F}} = z'\left(1 - 4\frac{\epsilon^2}{z'^2}\right)^{1/2}, \quad x_{\mathrm{F}} = z\left(1 - \frac{\epsilon^2}{z^2}\right), \quad (59)$$

$$z' = x_{\mathrm{F}}\left(1 + 4\frac{\epsilon^2}{x_{\mathrm{F}}^2}\right)^{1/2}, \quad z' = z\left(1 + \frac{\epsilon^2}{z^2}\right), \quad (60)$$

$$z = x_{\mathrm{F}}\frac{1}{2}\left[1 + \left(1 + 4\frac{\epsilon^2}{x_{\mathrm{F}}^2}\right)^{1/2}\right],$$

$$z = z'\frac{1}{2}\left[1 + \left(1 - 4\frac{\epsilon^2}{z'^2}\right)^{1/2}\right]. \quad (61)$$

If we start from, e.g., a cross-section evaluated in our formalism (we omit here the dependence on x and y)

$$\frac{\mathrm{d}\sigma}{\mathrm{d}z} \propto D_h(z), \quad (62)$$

the corresponding cross-section expressed as a function of x_{F} will be given by

$$\frac{\mathrm{d}\sigma}{\mathrm{d}x_{\mathrm{F}}} = \frac{\mathrm{d}z}{\mathrm{d}x_{\mathrm{F}}}\frac{\mathrm{d}\sigma}{\mathrm{d}z} \propto D_h[z(x_{\mathrm{F}})], \quad (63)$$

where, apart from the overall rescaling factor $\mathrm{d}z/\mathrm{d}x_{\mathrm{F}}$, one must keep into account that fragmentation functions, obtained in the variable z, are to be rescaled to the z value corresponding to x_{F}.

In variables like polarizations, given as ratios of two cross-sections, the overall rescaling factors cancel out and the remaining effect is the rescaling between the two variables in the fragmentation functions, according to (59)–(61).

Of course, if the average value of the polarization over a given kinematical region is required, the appropriate overall rescaling factors, like $\mathrm{d}z/\mathrm{d}x_{\mathrm{F}}$ in (63), have to be taken into account in the kinematical integrations.

References

1. M. Anselmino, M. Boglione, J. Hansson, F. Murgia, Phys. Rev. D **54**, 828 (1996)
2. R.L. Jaffe, Phys. Rev. D **54**, 6581 (1996)
3. J. Ellis, D. Kharzeev, A. Kotzinian, Z. Phys. C **69**, 467 (1996)
4. D. de Florian, M. Stratmann, W. Vogelsang, Phys. Rev. D **57**, 5811 (1998)
5. A. Kotzinian, A. Bravar, D. von Harrach, Eur. Phys. J. C **2**, 329 (1998)
6. A. Kotzinian, talk at the VII Workshop on High Energy Spin Physics (SPIN-97), 7–12 July 1997, Dubna, Russia; e-Print Archive: hep-ph/9709259
7. S.L. Belostotski, Nucl. Phys. B (Proc. Suppl.) **79**, 526 (1999)
8. D. Boer, R. Jakob, P.J. Mulders, Nucl. Phys. B **564**, 471 (2000)
9. C. Boros, J.T. Londergan, A.W. Thomas, Phys. Rev. D **61**, 014007 (2000)
10. D. Ashery, H.J. Lipkin, Phys. Lett. B **469**, 263 (1999)
11. B-Q. Ma, I. Schmidt, J. Soffer, J-Y. Yang, Eur. Phys. J. C **16**, 657 (2000); Phys. Rev. D **62**, 114009 (2000)
12. M. Anselmino, M. Boglione, F. Murgia, Phys. Lett. B **481**, 253 (2000)
13. NOMAD Collaboration, P. Astier et al., Nucl. Phys. B **588**, 3 (2000); Nucl. Phys. B **605**, 3 (2001)
14. M. Glück, E. Reya, A. Vogt, Z. Phys. C **67**, 433 (1995)
15. M. Glück, E. Reya, M. Stratmann, W. Vogelsang, Phys. Rev. D **53**, 4775 (1996)
16. D. Indumathi, H.S. Mani, A. Rastogi, Phys. Rev. D **58**, 094014 (1998)
17. M.L. Mangano et al., CERN report CERN-TH/2001-131, e-Print Archive: hep-ex/0105155
18. M. Anselmino, M. Boglione, U. D'Alesio, E. Leader, F. Murgia, Phys. Lett. B **509**, 246 (2001)
19. D.V. Naumov, private communication